Journal of Power Sources 188 (2009) 546–551

Contents lists available at ScienceDirect

Journal of Power Sources

journal homepage: www.elsevier.com/locate/jpowsour

Electrochemical properties of Li_2ZrO_3-coated silicon/graphite/carbon composite as anode material for lithium ion batteries

Ming-Qi Li[a,b,c], Mei-Zhen Qu[a], Xiao-Ying He[b], Zuo-Long Yu[a,*]

[a] Chengdu Organic Chemical Institute of Chinese Academy of Sciences, Chengdu 610041, China
[b] College of Chemistry and Chemical Engineering, China West Normal University, Nanchong 637002, China
[c] Graduate University of the Chinese Academy of Sciences, Beijing 100049, China

ARTICLE INFO

Article history:
Received 2 August 2008
Received in revised form 1 December 2008
Accepted 2 December 2008
Available online 7 December 2008

Keywords:
Silicon/graphite/disordered carbon
Li_2ZrO_3
Lithium ion batteries
Anode material
Electrochemical performance

ABSTRACT

Silicon/graphite/disordered carbon (Si/G/DC) is coated by Li_2ZrO_3 using $Zr(NO_3)_4{\cdot}5H_2O$ and $CH_3COOLi{\cdot}2H_2O$ as coating reagents. X-ray diffraction (XRD), scanning electron microscopy (SEM) and transmission electron microscopy (TEM) are used to characterize Li_2ZrO_3-coated Si/G/DC composite. The Li_2ZrO_3-coated Si/G/DC composite exhibits a high reversible capacity with no capacity fading from 2nd to 70th cycle, indicating its excellent cycleability when used as anode materials for lithium ion batteries. A compact and stable solid-electrolyte interphase (SEI) layer is formed on the surface of Li_2ZrO_3-coated Si/G/DC electrode. Analysis of electrochemical impedance spectra (EIS) shows that the resistance of the coated material exhibits less variation during cycling, which indicates the integrity of electrode structure is kept during cycling. XPS shows that F and P elements do not appear in the SEI layers of Li_2ZrO_3-coated Si/G/DC electrode, while they have a relatively high content in SEI layers of Si/G/DC electrode. The improvement of Li_2ZrO_3-coated Si/G/DC is attributed to the decrease of lithium insertion depth and the formation of stable SEI film.

1. Introduction

Lithium ion batteries containing graphite anodes are now the most widely used power sources for portable electronic devices. For commercial applications, however, lithium ion batteries with high specific energy density are in increasing demand. Recently, various anode materials have been proposed to overcome the limited capacity of graphite (372 mAh g^{-1}). Much attention has been paid to silicon-based anode materials because silicon has the high specific capacity of 3579 mAh g^{-1} at room temperature [1]. Unfortunately, Si-based electrodes typically suffer from poor capacity retention. In order to improve the cycleability of silicon-based materials, many attempts have been made [2–16]. Among them, silicon–graphite–carbon composites in which ultra fine silicon particles are dispersed uniformly in a ductile matrix of graphite and the mixtures are coated with carbon, were thought to be a promising anode material for high-capacity rechargeable lithium batteries. However, silicon–graphite–carbon composites without special cycling procedures during charge–discharge cycles still show bad capacity retention with comparison to graphite. Recently, some studies are interesting. For example, Beattie' study [17] shows that Si-based electrodes with a relatively low nano-Si content can accommodate large changes in volume due to particle lithiation and delithiation, while persistent irreversible decomposition of electrolyte is observed in all Si-based electrodes. It is reported that VC-containing electrolyte, in which the discharge/charge depth of electrode was reduced for the high polarization of electrode arising from denser or thicker SEI layer, can significantly enhance the cycleability of Si-based electrodes [18]. It was also found by Osakak et al. [19] that approximately 1 wt.% Si contained in the negative electrode was dissolved in the non-aqueous electrolyte and a large amount of Si-containing compound was detected together with Li-containing inorganic and organic compounds in the coating film formed on the surface of electrode active material. Based on these investigations, it is speculated that the poor cycleability for Si-based materials originates from not only its large volume change during cycling, but also side reactions including the dissolution of electrode materials and the decomposition of electrolyte. It is expected that if the lithium insertion into Si-based materials and side reactions can be controlled simultaneously to some extend, the cycleability of Si-based materials will be improved. In this paper, a Li_2ZrO_3 layer was used to coat Si/G/DC material to verify our speculation. It is well known that Li_2ZrO_3 is generally stable and chemical inert in common non-aqueous electrolyte, and quite suitable as coating shell to protect the electrode material. Moreover, it can decrease discharge/charge capacity for its electron blocking effect when its thickness increases to some extend. In addition, it may also serve

* Corresponding author. Tel.: +86 1388171629 fax: +86 2885215069.
E-mail address: lmingq888@163.com (Z.-L. Yu).

0378-7753/$ – see front matter © 2008 Elsevier B.V. All rights reserved.
doi:10.1016/j.jpowsour.2008.12.010

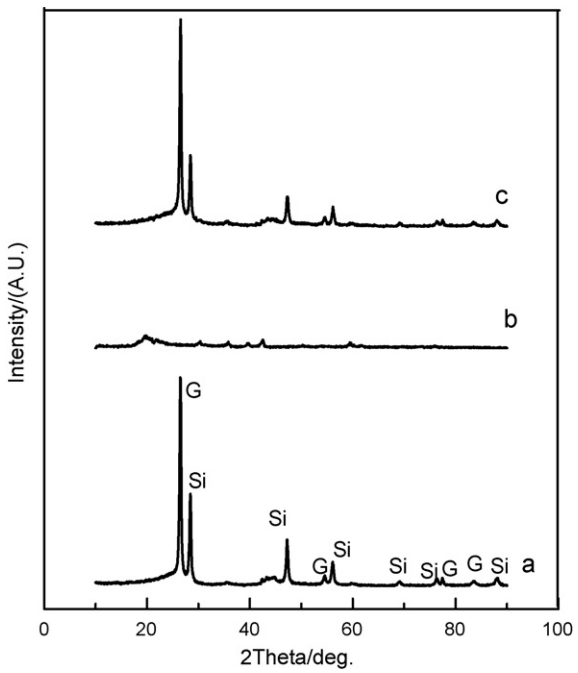

Fig. 1. XRD patterns of samples: (a) Si/G/DC, (b) Li_2ZrO_3 and (c) Li_2ZrO_3-coated Si/G/DC.

to scavenge and neutralize any HF species present in the electrolyte [20]. Based on its advantageous properties, Li_2ZrO_3 was selected as the coating layer for Si/G/DC material. Experiments showed that the Li_2ZrO_3 coating significantly improved the electrochemical performance of Si/G/DC material.

2. Experimental

Preparation of the Si/G/DC composite: 2 g pitch was dissolved in 15 ml trichloroethylene to form a homogeneous solution. Natural graphite (1.2 g, 2 μm), Si (0.6 g, 50 nm), and pitch solution were loaded into a stainless steel (SS) vial containing 10 mm diameter SS balls with a mass ratio of 15:1 inside an argon filled glove box in order to minimize the oxidation of starting materials. The pitch solution submerges the starting precursors and the milling media completely inside the vial. Mixtures of graphite, silicon, and pitch solution were subjected to mechanical milling up to 18 h using a planetary ball mill, and then dried in air at 383 K. The powders were annealed isothermally at 1273 K for 2 h in an ultra high purify argon gas using a heating rate of 10 K min^{-1} and a flow rate of 100 ml min^{-1}. The resulting composites (labelled as Si/G/DC) were further ground by a planetary ball mill at a rotation speed of 500 rpm for 1 h and sieved by 300-mesh sifter.

To coat Si/G/DC with Li_2ZrO_3, $Zr(NO_3)_4{\cdot}5H_2O$ and $CH_3COOLi{\cdot}2H_2O$ were used as coating reagents. In a typical experiment, 0.068 g $Zr(NO_3)_4{\cdot}5H_2O$ and 0.0326 g $CH_3COOLi{\cdot}2H_2O$ were dissolved in 40 ml ethanol in beaker, then 1.1979 g Si/G/DC was added to obtain 2 wt.% coated product. The beaker was maintained at 343 K under violent stirring until the solvent evaporated. The resulting powder was collected, dried, and finally calcined at 923 K for 5 h. For comparison, Li_2ZrO_3 without Si/G/DC was also prepared by the same procedure.

The powders produced were characterized by X-ray diffractometer (XRD, X'Pert MPD X), scanning electron microscope (SEM, JEOL 5900LV) and transmission electron microscope (TEM, JEM-100CX). In addition, SEM was also used to observe the change of electrodes in morphology and microstructure after given cycles. XPS was used to investigate the chemical component of the SEI layer

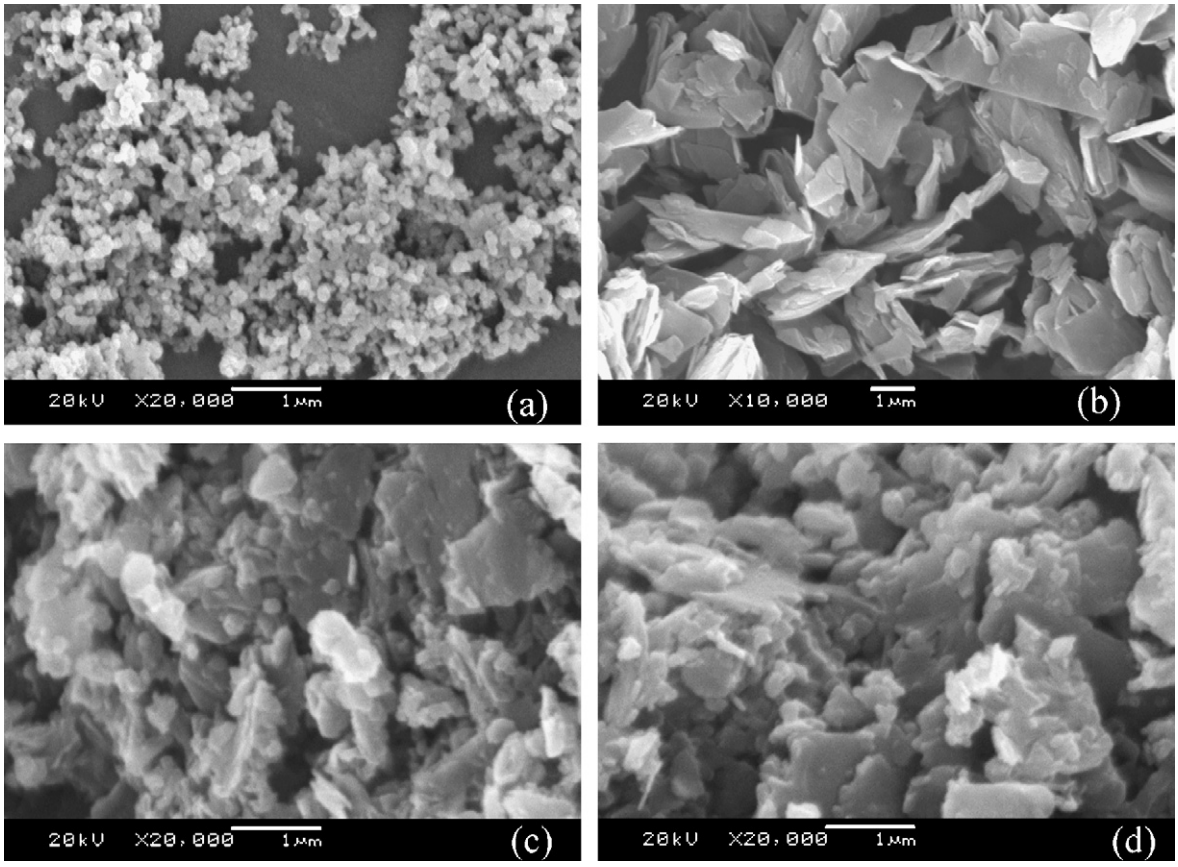

Fig. 2. SEM micrographs of samples: (a) Si, (b) graphite, (c) Si/G/DC and (d) Li_2ZrO_3-coated Si/G/DC.

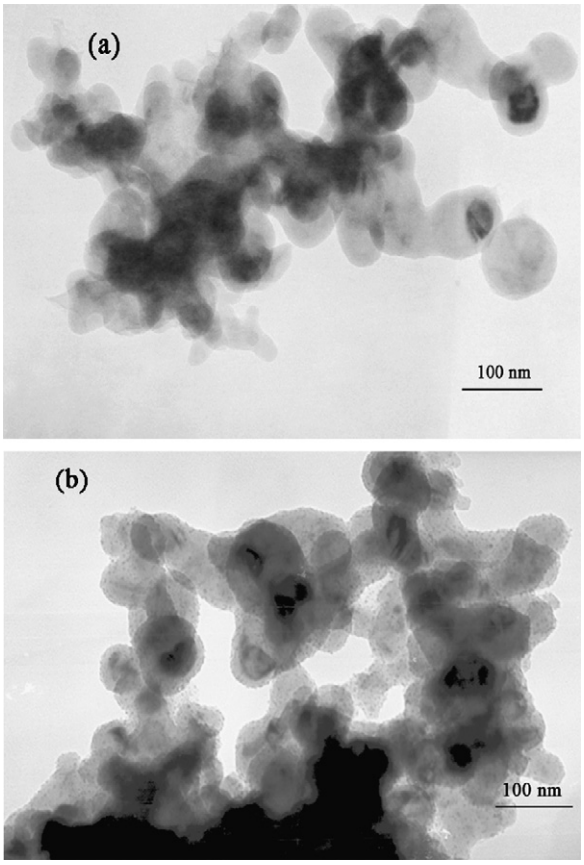

Fig. 3. TEM micrographs of samples: (a) Si/G/DC and (b) Li_2ZrO_3-coated Si/G/DC.

on the surface of electrode. The electrodes were prepared by pasting an aqueous slurry containing 85 wt.% composite powder, 5 wt.% super P, 10 wt.% carboxymethyl cellulose (CMC) as a binder, on to a copper foil. The electrodes were then dried at 373 K for 12 h under vacuum and subsequently pressed. The electrolyte was 1 M $LiPF_6$ in EC/DMC/EMC (1:1:1, v/v/v) mixed solvents. 2016 coin cells were fabricated using a metallic lithium foil as a counter electrode. The cells were assembled in an argon filled glove box. The discharge and charge measurements were carried out on a Kingtian system. The cells were discharged (lithiation) and charged (delithiation) between 0.02 and 1.5 V versus Li/Li^+ at a constant current

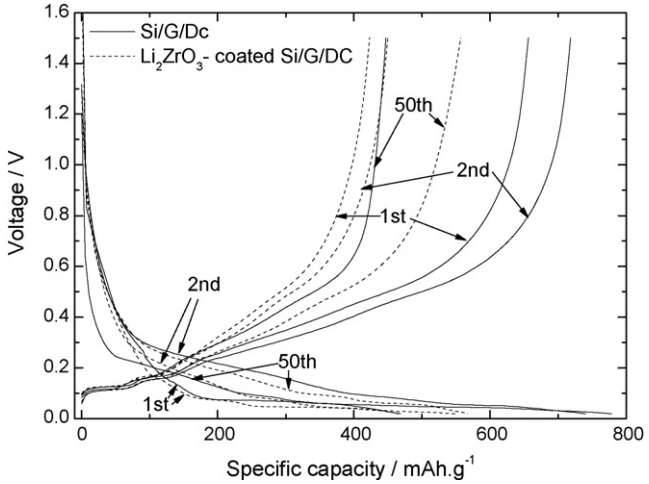

Fig. 4. Charge–discharge curves of Si/G/DC and Li_2ZrO_3-coated Si/G/DC electrode for 1st, 2nd and 50th cycle.

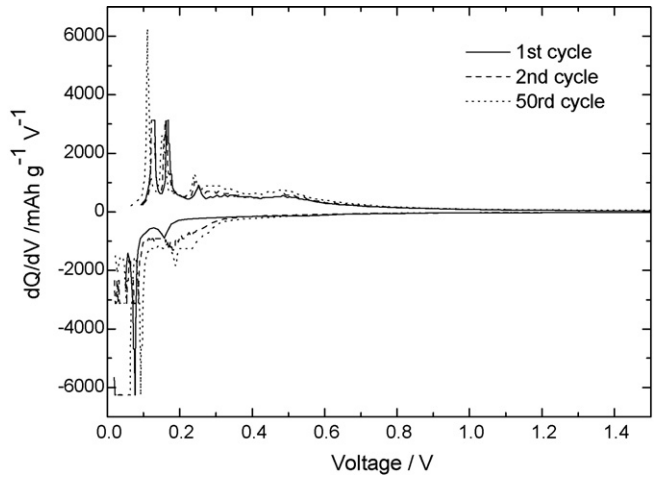

Fig. 5. Differential capacity vs. voltage curves of Li_2ZrO_3-coated Si/G/DC electrode for 1st, 2nd and 50th cycle.

density of 168 mA g^{-1}. The specific capacity of the Li_2ZrO_3-coated Si/G/DC/composite was calculated by using the entire mass of Si + G + DC + Li_2ZrO_3. Electrochemical impedance spectroscopy (EIS) measurements were carried out at M283 electrochemical workstation (America, EG&G corporation). The tests were performed after given cycles. The frequency used for the impedance measurements was 10 mHz to 100 kHz, and the signal amplitude was 5 mV.

3. Results and discussion

The XRD patterns of samples are shown in Fig. 1. Si/G/DC exists only the crystalline diffraction peaks of the silicon and graphite in addition to a broadened diffused peak at around $2\theta = 26^\circ$ that is attributable to the disordered carbon. There is no bulk SiO_2, SiC or Fe_xSi crystalline phase detected in Si/G/DC composites. Based on the 42% yield of pitch-C and no weight loss of Si and graphite, the composition of the Si/G/DC composite are estimated to be approximately G–21.1 wt.% Si–29.6 wt.% DC. There are a broad peak shape in the range of 17–24° and three weak peaks centered at 39.6°, 42.5° and 59.3° in the XRD of Li_2ZrO_3, which indicate the amorphous or nano-crystal character of Li_2ZrO_3, because crystallized Li_2ZrO_3 bulk is generally formed at temperature above 1023 K [21], while the peaks due to ZrO_2 are not found. Compared to Si/G/DC sample, there is no significant difference in the XRD of Li_2ZrO_3-coated

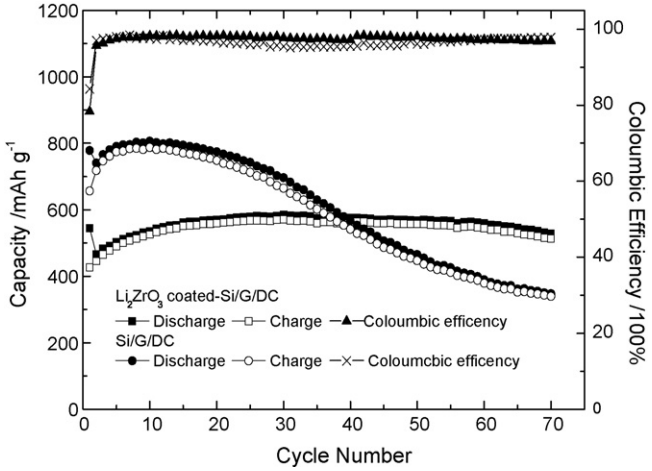

Fig. 6. Specific capacity vs. cycle number of Si/C/DC and Li_2ZrO_3-coated Si/G/DC cycled at a rate of 168 mAh g^{-1}.

Si/G/DC, which means no other bulk crystalline products are formed during coating Si/G/DC. In the XRD of Li_2ZrO_3-coated Si/G/DC composite, no distinct peaks due to Li_2ZrO_3 may result from the low content and the amorphous or nano-crystal character of Li_2ZrO_3.

In order to examine the microstructure of the composite particles, SEM and TEM analyses were conducted. Fig. 2 shows the SEM images of different samples. The SEM images of the nano-silicon and natural flake graphite, used to prepare the Si/G/DC composite materials, are also presented. The Si powders show a uniform particle-size distribution between 20 and 100 nm. The overall particle shape of graphite was thin and flat. From Fig. 2(c), nano-Si is homogeneously distributed in graphite matrix, which provides a buffer during the insertion/extraction of lithium ions, and Si/graphite particles are coated by the disordered carbon from pitch. In addition, Si/G/DC composite materials show clear surfaces and aculeated edges. After coating, the particles become more agglomerate and the edges become less discernable. Fig. 3 illustrates the TEM images of Li_2ZrO_3-coated Si/G/DC material. It is clearly seen that the surface of the particle is coated with a homogeneous layer, which comprises a large number of uniformly distributed protrudes of nano-crystals lithium zirconate according to XRD patterns, and there are more agglomerate particles after coating, indicating directly a successful coating operation [22].

The discharge/charge curves of Si/G/DC and Li_2ZrO_3-coated Si/G/DC composite materials are shown in Fig. 4. During the first insertion process, two electrodes present a distinct platform at around 0.20–0.02 V, which is mainly caused by the alloying process of silicon with lithium and the insertion of lithium ions into the carbon host. The slope at about 0.5 V corresponds to the irreversible decomposition of electrolyte, which results in the formation of SEI film on the electrode surface. During the first disinsertion process, the broad platform at around 0.25–0.6 V corresponds to the de-alloying reaction of lithium from the Li_xSi phase. However, the charge–discharge behaviors of Si/G/DC and Li_2ZrO_3-coated Si/G/DC display some obvious differences. Compared to Si/G/DC electrode, Li_2ZrO_3-coated Si/G/DC electrode demonstrates a lower intercalation voltage platform and a higher extraction voltage platform in the 1st cycle, which should be responsible for the reduced charge/discharge capacity of Li_2ZrO_3-coated Si/G/DC electrode. Moreover, the potential and the length of platforms for two electrodes present different changes with the increasing cycle number. From the 2nd cycle to the 50th cycle, the potential difference between lithium insertion platform and lithium extraction platform of Li_2ZrO_3-coated Si/G/DC electrode decreases and the length of platforms increases with the increasing of cycle number. However, the potential difference of Si/G/DC electrode decreases and then increase with the increasing of cycle number. In the 50th cycle, the potential difference between lithium insertion platform and lithium extraction of Si/G/DC electrode is much larger than that of Li_2ZrO_3-coated Si/G/DC electrode and the length of its platforms decreases largely. These results show that the conductive network of Li_2ZrO_3-coated Si/G/DC electrode is maintained during the prolonged cycling, while the microstructure of Si/G/DC electrode is destroyed severely.

Fig. 5 is the differential capacity plot of Li_2ZrO_3-coated Si/G/DC composite. It can be seen that Si and graphite are active. In the 1st cycle, the peak at 0.05 V corresponds to the lithium insertion reaction into nano-crystalline Si, while the peaks at 0.252 and 0.485 V are lithium disinsertion reaction from Li_xSi. There are peaks present for graphite at 0.157, 0.077, 0.05 0.128 and 0.163 V. The appearance of peaks corresponding to 0.074 and 0.217–0.344 V suggest that the crystalline Si transforms to amorphous Si after the 1st cycle, while the peaks for graphite have no significant change except of lithium insertion peak shifting positively ~15 mV. The peak intensity due

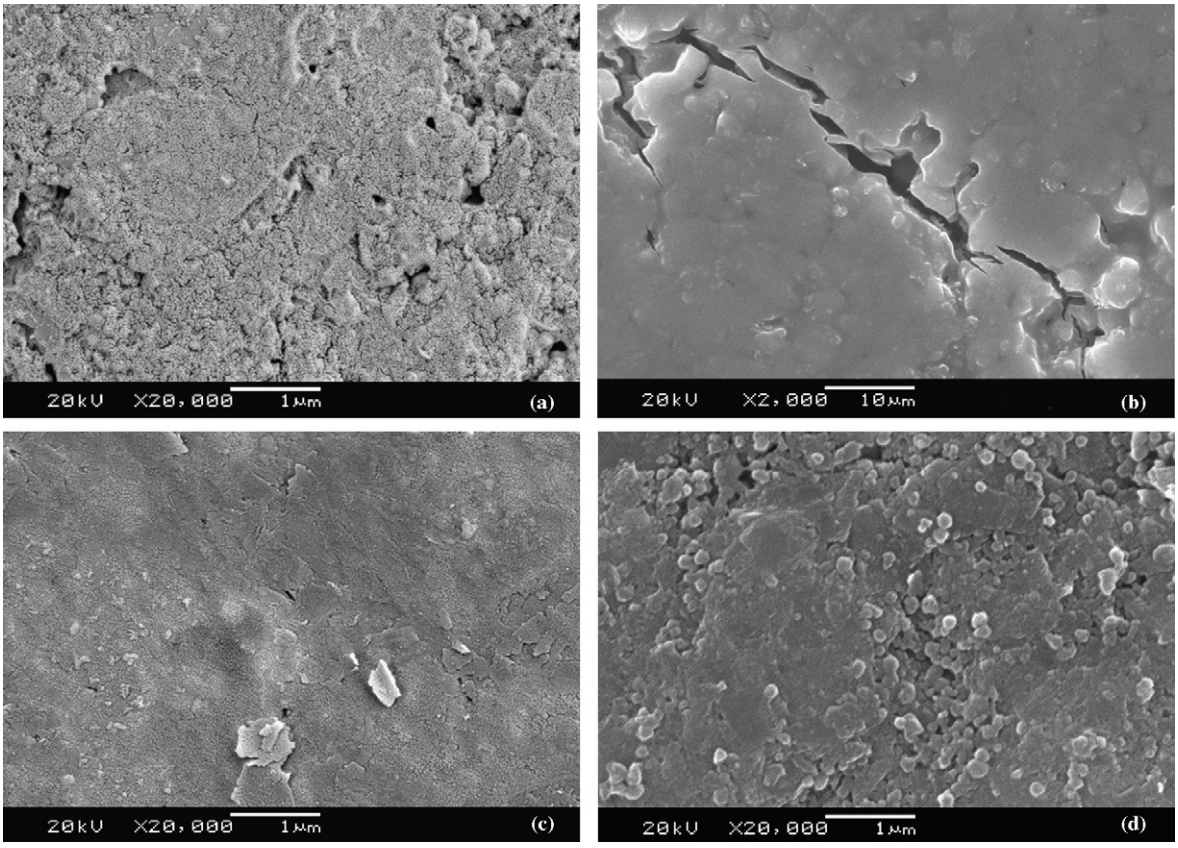

Fig. 7. SEM images of composite electrode. Si/G/DC: after 1st cycle (a) and after 70th cycle (b). Li_2ZrO_3-coated Si/G/DC: after 1st cycle (c) and after 70th cycle (d).

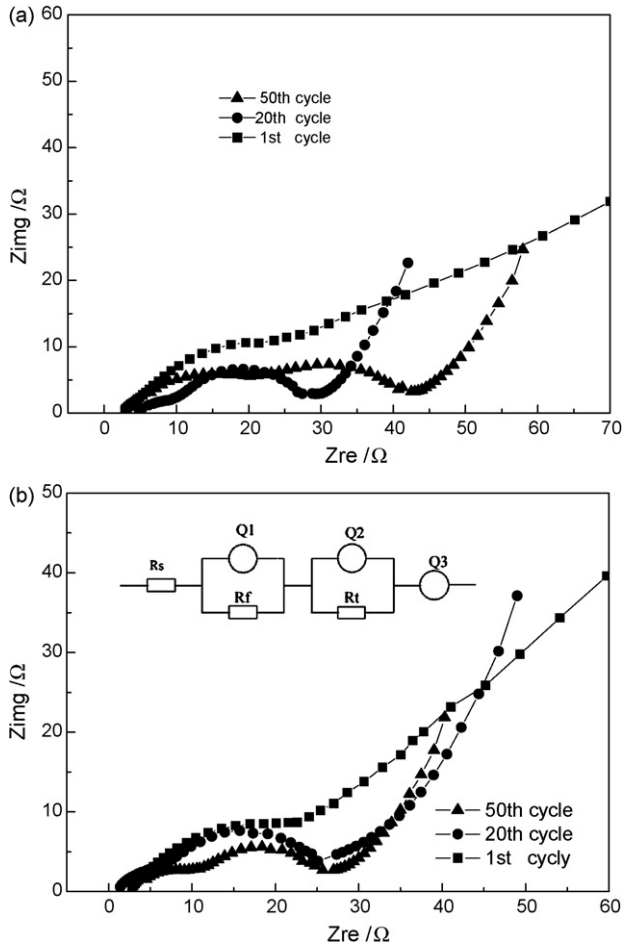

Fig. 8. Electrochemical impedance spectra of Si/G/DC electrode (a) and Li_2ZrO_3-coated Si/G/DC electrode (b) at different cycle stages. Inset: the schematic representation of equivalent circuit.

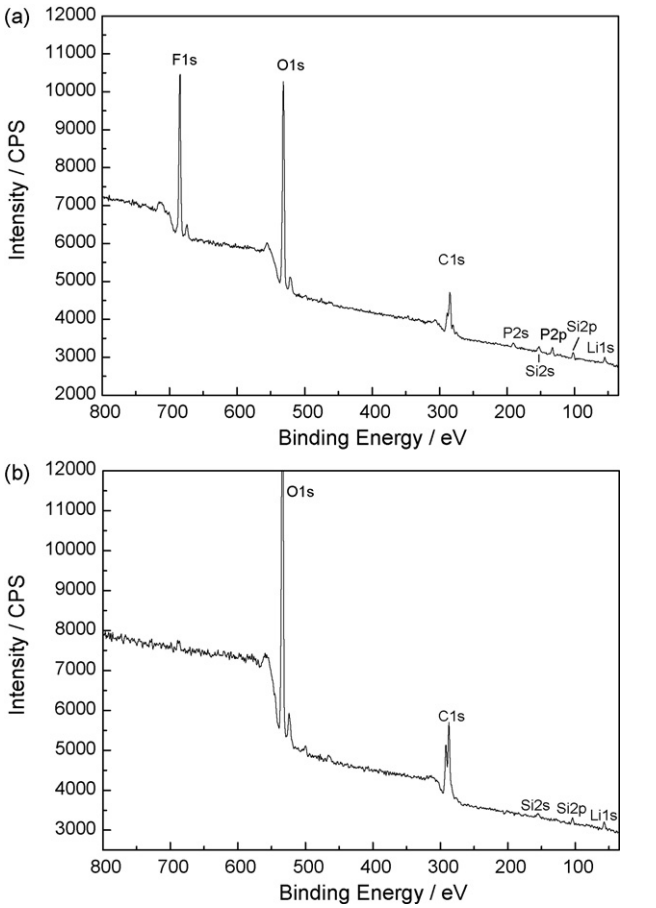

Fig. 9. XPS spectra for SEI layers of Si/G/DC (a) and Li_2ZrO_3-coated Si/G/DC electrode (b) after 1st cycle.

to the reaction of Li ion with amorphous Si does not decrease even after the 50th cycle, which suggests the excellent capacity retention of the composite.

Fig. 6 shows the variation of specific capacity versus cycle number of Si/G/DC and Li_2ZrO_3-coated Si/G/DC cycled at a constant current of 168 mA g^{-1}. The Si/G/DC composite shows an initial discharge capacity ~825 mAh g^{-1} with an irreversible loss of 215 mAh g^{-1}. However, the capacity of Si/G/DC rapidly decreases with increasing cycle number after 20th cycle. In contrast, Li_2ZrO_3-coated Si/G/DC composite exhibits excellent capacity retention, while it displays a relatively low initial discharge (544 mAh g^{-1}, volumetric energy density is ~1062 mAh cm^{-3}) with an irreversible loss of 118 mAh g^{-1}. The reversible capacity of Li_2ZrO_3-coated Si/G/DC composite increases with subsequent cycles and after the 10th cycle the reversible capacity increases to ~530 mAh g^{-1}, which is maintained upon cycling up to 70 cycles. In addition, Li_2ZrO_3-coated Si/G/DC composite exhibits a high and stable coulomb efficiency, with averaged ~98% coulomb efficiency after 1st cycle. However, although the irreversible capacity of Si/G/DC material descends from 215 to 118 mAh g^{-1} after coating, the decreased lithium insertion capacity of Li_2ZrO_3-coated Si/G/DC leads to increasing the ratio of irreversible capacity in total capacity. As a result, the first coulombic efficiency of Li_2ZrO_3-coated Si/G/DC is lower than that of Si/G/DC.In order to shed the light on the enhanced electrochemical performance of material via coating, the morphological changes of the composite electrodes after different cycles were examined by SEM (Fig. 7). After the 1st cycle, the surfaces of Si/G/DC and Li_2ZrO_3-coated Si/G/DC electrode display some significant difference. As shown in Fig. 7(a), the SEI layers formed on the Si/G/DC electrode surface are porous and have some fine cracks, suggesting SEI film formed on the Si/G/DC electrode surface is not compact and the electrode structure has been destroyed locally for large volume change. In contrast, relatively homogeneous and compact SEI layers are observed on the surface of Li_2ZrO_3-coated Si/G/DC electrode and no crack appears. After 70 cycles, large fracture appears in Si/G/DC electrode, while there appears to be no significant change in microstructure of Li_2ZrO_3-coated Si/G/DC composite electrode (Fig. 7(d)). These results indicate that Li_2ZrO_3 coating plays an important role in forming compact SEI layer and protecting the integrity of electrode structure. Since the final Si/G/DC composite was ground by ball mill, it was unavoidable that some silicon and graphite particles were bared on the surface of Si/G/DC composite. It was reported that when the silicon particles contact with the electrolyte directly, polymer-like porous substance will be formed on the surface of silicon particles, which prevents the formation of solid-electrolyte interface passivation layer on the silicon surface [23]. In contrast, because Li_2ZrO_3 coating on Si/G/DC composite prevents bared silicon from exposing to electrolyte, stable SEI layers may be formed. Therefore, the improvement of Li_2ZrO_3-coated Si/G/DC composite in the cyclic performance is attributed to the fact that Li_2ZrO_3 decreases the degree of lithium insertion into electrode materials and ameliorates the surface characteristics of Si/G/DC.

Electrochemical impedance spectrum (EIS) was also applied to analyze the evolution of electrode/electrolyte interface. The corresponding Nyquist plots were given in Fig. 8. The intercept at the

Table 1
Iterated parameters using equivalent circuit in Fig. 8.

	Si/G/DC			Coated Si/G/DC		
	1st	20th	50th	1st	20th	50th
R_s (Ω)	2.93	4.50	4.70	2.90	3.40	4.65
R_f (Ω)	2.81	7.37	15.88	3.54	6.33	7.21
R_{ct} (Ω)	15.52	17.02	22.29	13.92	15.17	15.72

Table 2
Atomic concentration of various elements in SEI layers of Si/G/DC and Li_2ZrO_3-coated Si/G/DC electrode.

	Element (%)					
	C	O	Si	F	P	Li
Si/G/DC	23.7	29.7	2.2	11.1	1.9	31.4
Coated Si/G/DC	34.9	23.9	1.9	0	0	39.2

Z_{re} axis in high frequency refers to R_s, which includes electrolyte solution resistance, electric contacts resistance, and ion conductive resistance. The semicircle in the high frequency range corresponds to the surface film resistance (R_f); the semicircle in the middle frequency range reflects the charge transfer resistance (R_{ct}); and the sloping line in the lower frequency represents lithium ion diffusion resistance in electrode bulk, namely the Warburg impedance. Non-linear least squares fitting procedure was used to iterate the impedance data applying the inset equivalent circuit in Fig. 8, in which constant phase element (Q) is used to substitute capacitance of electric double layer and Warburg impedance for the dispersion effect appearing in Nyquist plots, and the results are listed in Table 1. After 1st cycle, R_f of the Li_2ZrO_3-coated Si/G/DC is bigger than that of Si/G/DC, which implies the SEI film formed on the Li_2ZrO_3-coated Si/G/DC surface is more compact or thicker. In general, the R_{ct} and R_f of the Li_2ZrO_3-coated Si/G/DC show relatively smaller changes with comparison to those of Si/G/DC. The R_f of Si/G/DC after 50th cycle is higher almost five times than that of Si/G/DC after 1st cycle, while the R_f of Li_2ZrO_3-coated Si/G/DC simply increases one time from 1st cycle to 50th cycle. Since Si/G/DC electrode cannot accommodate the large volume change in prolonged cycling, new SEI film will form constantly on the fresh surface of active particles from the cracking of electrode in each cycle, which results in thickening SEI film and increasing R_f after repeating cycling. In contrast, Li_2ZrO_3-coated Si/G/DC electrode structure is not destroyed upon whole cycling so that the thickness of SEI film has no significant change. The R_{ct} of Si/G/DC increases ~7 Ω from 1st to 50th cycle, while that of the coated one only increases about 2 Ω, suggesting that the conductive network structure of Li_2ZrO_3-coated Si/G/DC is not destroyed upon cycling. These results are in good agreement with the SEM images shown in Fig. 7.

In order to obtain information on the chemical component of the SEI layer, XPS of the SEI layers formed on two kinds of electrode surface were examined after the 1st cycle (Fig. 9). The peaks at 55, 102, 133.2, 280–290, 531.6 and 684.7 eV are due to Li_{1s}, $Si_{2p3/2}$, $P_{2p3/2}$, C_{1s}, O_{1s} and F_{1s}, respectively. Among them, $Si_{2p3/2}$ at 102 eV should be assigned to SiO_x, which has also been found in SEI layer in Si electrode [24]. However, the formation mechanism of SiO_x in the SEI layer on Si-based materials is still unknown. Based on atom sensitivity factor, semiquantitative analysis results of the XPS spectra are listed in Table 2. It may be seen that their chemical components are different. F and P elements, which come from the side reactions of $LiPF_6$, are not detected in SEI layers of Li_2ZrO_3-coated Si/G/DC electrode, while the atomic concentration of F and P elements in SEI layers of Si/G/DC electrode are as high as 11.1 and 1.9%, respectively. A high content of LiF in SEI layers is unfavorable to the formation of compact SEI film and the electrochemical performance of electrode [25]. Moreover, although silicon oxide appears in the SEI layers of Li_2ZrO_3-coated Si/G/DC and Si/G/DC electrodes, the atom concentration of Si in the SEI layer of the former is lower than that in the SEI layer of the latter. These results show that Li_2ZrO_3 has positive effect on suppressing the side reactions of $LiPF_6$.

4. Conclusions

A Li_2ZrO_3 layer was successfully coated on the surface of Si/G/DC material. The Li_2ZrO_3 coating layer is helpful to form stable and compact SEI layer on the surface of electrode material and decrease the depth of lithium insertion into Si/G/DC electrode, which alleviates the mechanical stress of electrode and keeps the integrity of electrode. As a result, the electrochemical performance of Si/G/DC material was significantly improved.

Acknowledgments

This research was supported by the Ministry of Energy and Technology of the People's Public of China (No. 2006CB932703), Chinese Academy of Sciences (Grant No. KJCX-YW-M01) and Zhongke Laifang Energy and Technology Co. Ltd.

References

[1] M.N. Obrovac, L. Christensen, Electrochem. Solid-State Lett. 7 (2004) 93–96.
[2] U. Kasavajjula, C.S. Wang, A.J. Appleby, J. Power Sources 163 (2007) 1003–1039.
[3] A. Timmons, A.D.W. Todd, S.D. Mead, G.H. Carey, R.J. Sanderson, R.E. Mar, J.R. Dahn, J. Electrochem. Soc. 154 (2007) 865–874.
[4] J.H. Lee, W.J. Kim, J.Y. Kim, S.H. Lim, S.M. Lee, J. Power Sources 176 (2008) 353–358.
[5] C.K. Chan, H.L. Peng, G. Liu, K. Mcilwrath, X.F. Zhang, Nat. Nanotechnol. 3 (2008) 31–35.
[6] D.K. Kang, J.A. Corno, J.L. Gole, H.C. Shin, J. Electrochem. Soc. 155 (2008) 276–281.
[7] C.H. Doh, C.W. Park, H.M. Shin, D.H. Kim, Y.D. Chung, S.I. Moon, B.S. Jin, H.S. Kim, A. Veluchamy, J. Power Sources 179 (2008) 367–370.
[8] S.H. Ng, J. Wang, D. Wexler, S.Y. Chew, H.K. Liu, J. Phys. Chem. C 111 (2007) 11131–11138.
[9] J.H. Kim, H.J. Sohn, H. Kim, G. Jeong, W. Choi, J. Power Sources 170 (2007) 456–459.
[10] Y. Zheng, J. Yang, J. Wang, Y. Nuli, Electrochim. Acta 52 (2007) 5863–5867.
[11] Y.M. Kang, M.S. Park, J.Y. Lee, H.K. Liu, Carbon 45 (2007) 1928–1933.
[12] L. Lacroix-orio, M. Tillard, D. Zitoun, C. Belin, Chem. Mater. 20 (2008) 1212–1214.
[13] W.R. Liu, N.L. Wu, D.T. Shieh, H.C. Wu, M.H. Yang, C. Korepp, J.O. Besenhard, M. Winter, J. Electrochem. Soc. 154 (2007) 97–102.
[14] B. Lestriez, S. Bahri, I. Sandu, L. Roue, D. Guyomard, Electrochem. Commun. 9 (2007) 2801–2806.
[15] Y. Kwon, J. Cho, Chem. Commun. 9 (2008) 1109–1111.
[16] Z.S. Wen, F. Tian, J.C. Sun, S.J. Ji, J.Y. Xie, Rare Met. 27 (2008) 170–174.
[17] S.D. Beattie, D. Larcher, M. Morcrette, B. Simon, J.M. Tarascon, J. Electrochem. Soc. 155 (2008) 158–163.
[18] Y.S. Hu, R.D. Cakan, M.M. Titirici, J.O. Müller, R. Schögl, M. Antonietti, J. Maier, Angew. Chem. Int. Ed. 47 (2008) 1645–1649.
[19] T.S. Osaka, Y.B. Osaka, M.U. Osaka, US 2006/0286458 A1.
[20] M.M. Thackeray, C.S. Johnson, J.S. Kim, K.C. Lauzze, J.T. Vaughey, N. Dietz, D. Abraham, S.A. Hackney, W. Zeltner, M.A. Anderson, Electrochem. Commun. 5 (2003) 752–758.
[21] D. Cruz, H. Pfeiffer, S. Bulbulian, Solid State Sci. 8 (2006) 470–475.
[22] J. Ni, H. Zhou, J. Chen, X. Zhang, Electrochim. Acta 53 (2008) 3075–3083.
[23] X. Wu, Z. Wang, L. Chen, X. Huang, Electrochem. Commun. 5 (2003) 935–939.
[24] L.B. Chen, K. Wang, X.H. Xie, J.Y. Xie, J. Power Sources 174 (2007) 538–543.
[25] A.M. Andersson, K. Edstrom, J. Electrochem. Soc. 148 (2001) 1100–1109.